

Decentralized Control with Minimum Dissolved Oxygen Guaranties in Aerobic Fed-Batch Cultivations

Sebastián Nuñez,* Fabricio Garelli, and Hernán De Battista

CONICET and LEICI, Facultad de Ingeniería, Universidad Nacional de La Plata, Calle 48 esq. 116 s/n, La Plata, Buenos Aires 1900, Argentina

ABSTRACT: In this work, a control strategy to guarantee a minimum dissolved oxygen concentration in aerobic fed-batch bioprocesses is proposed. The strategy is equally applicable to avoid low oxygen concentrations that might be detrimental for metabolites production, to prevent metabolic changes and to maintain an oxygen level in the culture compatible with the desired growth rate during the growing phase of the process. It essentially consists in adapting the set-point of the feeding controller to cope with faults and saturation in the oxygen regulation subsystem. The idea behind this adaptation is to manipulate, when necessary, the oxygen consumption in such a way that the oxygen in the culture is maintained above a prescribed threshold. The algorithm is based on sliding mode techniques, and its main features are as follows: simplicity, robustness to process uncertainties, easy implementation, and versatility to be combined with different dissolved oxygen and feeding controllers. The method is assessed numerically in a fed-batch growth phase of *Pichia pastoris* where an oxygen shortage leads to excessive glycerol accumulation.

1. INTRODUCTION

Biotechnological processes are widely used for the production of pharmaceutical products, agricultural products, and several chemicals compounds. An important class of such processes are the aerobic ones, in which microorganisms need oxygen for growth, maintenance, and product synthesis.

The most popular mode of operation of bioreactors has been the fed-batch mode where the substrate is progressively fed to the reactor. This mode has the potential advantage of avoiding substrate overfeeding, which can inhibit the microbial growth and product formation.¹ Although fed-batch operation is often preferred, fed-batch cultures are very difficult to control because of the nonlinear behavior, scarce online measurements available for feedback, and strongly time-varying parameters.² Besides, the optimization of the feed rate is not trivial because it is a dynamical problem subjected to constraints on both the state and the control variables.³ In comparison to continuous cultivation, convergence speed and robustness of the control system is of primary importance in fed-batch reactors given the shorter duration of the cultivation.

During the growth phase of fed-batch processes, a substrate feeding with exponential profile is usually supplied to the reactor in order to maintain a desired specific growth rate while avoiding substrate accumulation. Specific growth rate regulation is often desired also to optimize process productivity by keeping microorganisms in a given physiological state.^{4,5} This operation strategy leads to an exponential growth of biomass which in turn produces exponential oxygen consumption. That is why oxygen limitation is very common under high cell density conditions in aerobic fed-batch processes. Oxygen shortage during growth rate regulation usually results in substrate accumulation, possibly causing process instability. Additionally, low oxygen in the culture may lead to metabolic changes in the microorganisms and byproducts formation. For instance, in oxygen-limited cultivations of *Pichia pastoris* on glucose or glycerol, fermentative byproducts such as ethanol

may have a negative impact on foreign protein expressions.⁶ A similar situation occurs for facultative organisms (e.g., *Saccharomyces cerevisiae* and *Escherichia coli*) since they can switch to anaerobic metabolism and accumulate toxic metabolites.

In this work, we present a method to adjust the feeding law of an aerobic fed-batch process so as to guarantee an appropriate aerobic condition. A decentralized control structure of the process is considered as a starting point. On the one hand, the dissolved oxygen (DO) is controlled in closed-loop manipulating the aeration. On the other hand, the feeding flow is controlled, either in open-loop or closed-loop, to regulate another variable such as the specific growth rate. A serious problem arises in this control structure when the aeration actuator reaches its operation limit, which typically occurs at the end of the process. In fact, in that case the aeration subsystem is not able to regulate DO anymore, which may drop to low values. In parallel, the feeding flow controller overfeeds the reactor since it does not take account of the DO shortage. The proposed method, which is inspired on previous ideas of the authors regarding multivariable process control,⁷ essentially consists in adding an auxiliary loop to the feeding law. This loop becomes active when the DO concentration is reaching a user-defined level and automatically switches off when the risk of falling below this level disappears. While it is active, a sliding mode (SM) algorithm adjusts the feeding flow to reduce the oxygen consumption in such a way that the DO remains within suitable values.

The method is assessed numerically in a fed-batch growth phase of *P. pastoris* where an oxygen shortage leads to excessive

Received: July 4, 2013

Revised: November 18, 2013

Accepted: November 20, 2013

Published: November 20, 2013

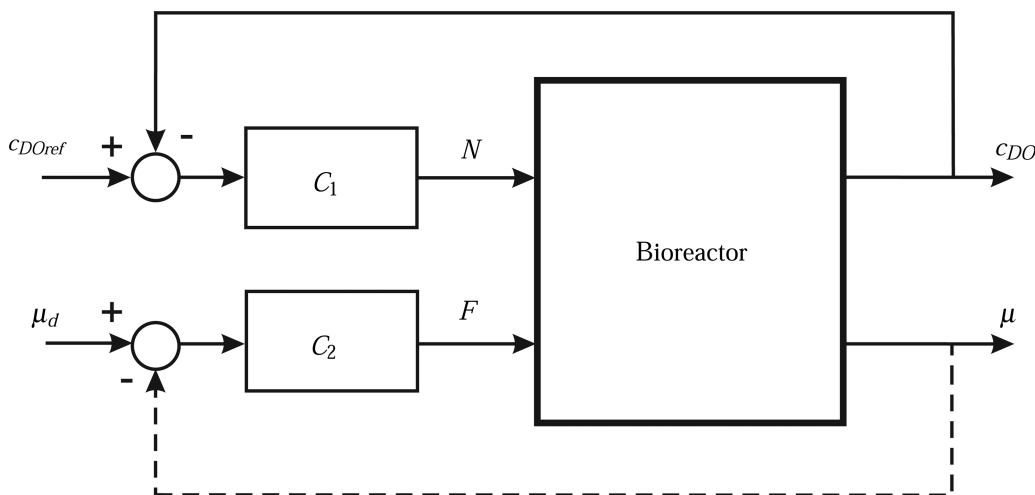


Figure 1. Decentralized control structure of the aerobic bioprocess: DO controller (C_1) and feeding law controller (C_2).

glycerol accumulation. Different scenarios are considered including DO control dysfunction due to actuator faults and saturation and open- and closed-loop control of the feeding flow.

2. PRELIMINARIES AND PROBLEM STATEMENT

2.1. Bioprocess Model. The following state equations describe the continuous model of a *P. pastoris* culture in a well-mixed stirred tank⁸

$$\dot{x} = \left(\mu - \frac{F}{v} \right) x \quad (1)$$

$$\dot{s} = -q_s x + (S_i - s) \frac{F}{v} \quad (2)$$

$$\dot{c}_{DO} = OTR - OUR - c_{DO} \frac{F}{v} \quad (3)$$

$$\dot{v} = F \quad (4)$$

where x , s , and c_{DO} are the biomass, substrate, and DO concentrations (g L^{-1}), respectively, and v is the liquid volume.

The specific growth rate $\mu(t)$ is commonly expressed as a product of factors.⁹ In this paper, the carbon source and the DO concentration in the liquid phase are considered the rate-limiting substrates^{8,10}

$$\mu(t) = \mu(s)\mu(c_{DO}) \quad (5)$$

Equation 5 corresponds to the 'interactive' case when the process is seen as a multiple-substrate bioprocess. The specific rates of substrate and oxygen consumption are described by¹¹

$$q_s = \frac{\mu}{Y_{xs}} + m_s \quad (6)$$

$$q_{O_2} = \frac{\mu}{Y_{xo}} + m_o \quad (7)$$

DO dynamics is mainly governed by the rates of oxygen transfer and uptake:

$$OTR = K_L a (c_{DO}^* - c_{DO}) \quad (8)$$

$$OUR = q_{O_2} x \quad (9)$$

$K_L a$ is affected by many factors like agitation speed, air flow rate, temperature, vessel geometry, and fluid characteristics.¹² Here, the nonlinear relation with the agitation speed (N) presented in Chung et al.¹³ is assumed

$$K_L a = \alpha N^\beta \quad (10)$$

with α and β being positive coefficients. Equation 10 can be seen as a simplified version of the correlation between $K_L a$ and the Power Number ($N^3 D^2$, with D being the impeller diameter) usually found in the literature.¹²

In order to exemplify the proposed feeding technique, the stirrer speed is assumed to be controlled by using a proportional + integral (PI) controller. Given an aeration level, the speed is increased if the DO level is lower than the set-point value. The stirrer speed is constrained by its minimum and maximum speed values, that is $\{N_{min} \leq N \leq N_{max}\}$ rpm. Besides, environmental variables such as temperature and pH are assumed to be controlled by external control loops.

2.2. Problem Statement. The control scheme under consideration is presented in Figure 1. It depicts a decentralized control structure where the outputs c_{DO} and μ are controlled from the inputs N and F , respectively.

It has been reported that μ regulation is a control objective related to the physiological state of the cells, product formation, and product quality.¹⁴ In such a case, an exponential feeding law in $F(t)$ should be provided. The set-point μ_d is usually chosen as a compromise between the desired productivity, on the one hand, and the oxygen requirement and its negative effects due to byproducts formation, on the other hand. Since μ cannot be measured directly, two possibilities arise for the feeding loop:

1. The feeding rate follows an exponential time profile, leading to an open-loop feeding strategy.
2. An estimation ($\hat{\mu}$) is used in feeding controller C_2 , leading to closed-loop feeding strategy.

Note from eqs 3, 7, and 9 that an increase in μ gives a rise in the oxygen demand, which in turn can lead to a drop in DO. This situation is worse at the end of the process, when biomass quantity is higher. Thus, when the oxygen requirement is greater than the maximum OTR of the bioreactor, the DO may decrease to very low levels becoming the rate-limiting substrate. For example, a particular form of eq 5 for processes with Monod kinetics is

$$\mu(s, c_{DO}) = \mu_{max} \frac{s}{s + k_s} \frac{c_{DO}}{c_{DO} + k_o} \quad (11)$$

Figure 2 shows a plot of eq 11 with respect to substrate for different DO concentration values and depicts a possible set-

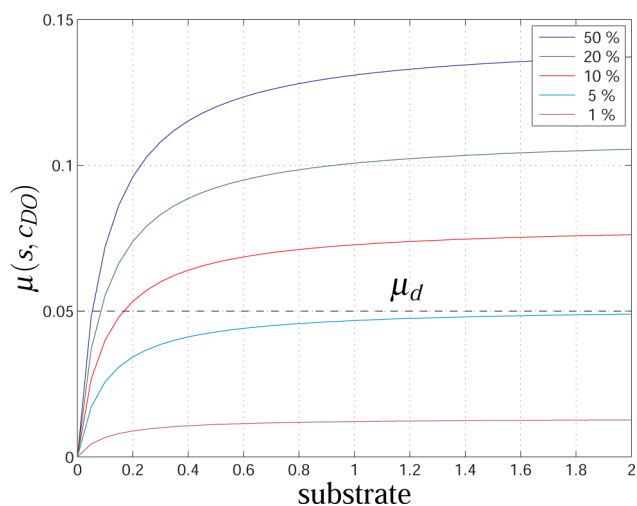


Figure 2. Specific growth rate vs substrate concentration for different DO values.

Table 1. Values Used in the Simulations^a

parameter	value	unit
Model Parameters for <i>P. pastoris</i>		
k_o	1	mg L ⁻¹
k_s	0.1	g L ⁻¹
μ_{max}	0.18	h ⁻¹
Y_{xo}	2.2	g g ⁻¹
Y_{xs}	0.5	g g ⁻¹
Bioreactor Parameters		
α	20	rpm ^{-β} h ⁻¹
β	0.5	-
N_{min}	320	rpm
N_{max}	1000	rpm
c_{DO}^*	8	mg L ⁻¹
k_p	2	rpm mg ⁻¹ L
k_i	0.2	rpm mg ⁻¹ L h ⁻¹
Growth Rate Controller (Section. 4.2)		
k_c	7.5	h
Auxiliary Loop Controller		
τ	0.25	h
α_f	1.0	rad/h
w_{SM}	μ_d	h ⁻¹

^aModel parameters of *P. pastoris* were taken from Oliveira et al.⁸

point value for μ (parameters taken from Table 1). It can be seen that the lower the DO concentration, the greater is the required substrate to achieve the desired growth rate. In practice, typical values for c_{DOref} are in the range [20–50]% of saturation value since these DO levels ensure that the growth-limiting substrate is the carbon source, and, therefore, the growth rate can be regulated with the feeding controller.

Usually, the required DO concentration is provided by manipulating the air flow rate and the stirrer speed.^{15–17} However, these inputs could not be used to guarantee the

necessary aerobic condition if their saturation values are reached (e.g., saturation of stirring speed). In such a case, the following problems may arise:

- the feeding law is unable to regulate μ at the desired set-point, causing undesired responses such as substrate accumulation in the culture.

- under anaerobic conditions, some microorganisms (e.g., *E. coli* and *S. cerevisiae*) can switch the metabolism to obtain energy, and growth-limiting byproducts may be excreted.^{18,19}

Although *P. pastoris* is not considered a fermentative yeast, results of ethanol accumulation under a high feed rate of glycerol have been reported.²⁰ Under oxygen limitation ethanol may have a negative impact on foreign protein expression, and therefore DO levels must be maintained sufficiently high.⁶ Moreover, during the production stage with methanol as the carbon source, oxygen is necessary given its relevant role in methanol oxidation pathway.²¹ The minimum value required for the production stage is around 20% of the saturation value.⁶

In the next section we propose the addition of a feeding adaptation algorithm with the aim of ensuring the aerobic condition above a given user-defined value.

3. DECENTRALIZED CONTROL WITH FEEDING ADAPTATION

The implementation of control algorithms in bioprocesses requires measurement of process variables. Environmental parameters such as temperature, pH, DO, and gaseous flow rates are commonly available for control purposes.²² However, biological variables are not always available, and this situation has led to the design and application of state observers.²³ In this section we consider a feeding adaptation block for application in both open- and closed-loop feeding strategies.

In the control structure presented in Figure 1, when oxygen consumption is lower than the maximum aeration capacity of the reactor, two variables are controlled from two inputs: DO is regulated by manipulating the stirrer speed, whereas μ is regulated with the substrate feeding rate. Due to the possibly exponential increase in oxygen demand, the main DO control loop may reach the maximum stirring speed. If this is the case, the variable to be controlled is μ subjected to the constraint in DO, which in fact is not regulated but bounded from below. Then, the policy is to shape the input flow via SM as close as possible to the pre-established one, while the constraint $c_{DO} \geq c_{DOmin}$ is fulfilled. Here c_{DOmin} is the minimum DO concentration allowed in the culture. This value is a design parameter and is reasonable to take it greater than or equal to the critical concentration of the culture, which depends on the microorganism and biotechnological objectives (e.g., to avoid undesired byproducts formation).

Figure 3 shows the proposed scheme for open-loop feeding strategies. The feeding adaptation block (F_{AD}) continuously updates the parameter μ_r of the exponential feeding law $F_{exp} = F_o e^{\mu_r t}$ as a function of the set-point μ_d , the measured value c_{DO} , and the lower bound c_{DOmin} .

Many processes require a robust regulation of μ . In Figure 4, the output μ_r of the feeding adaptation block is compared with an estimate given by a μ -observer. That is, in this case μ_r is the reference for the μ control loop. The growth rate can be estimated from related process measurements. For instance, from biomass and volume^{24,25} or OUR.²⁶ In block C_μ , a biomass proportional control law of the form $F_{expCL} = \lambda x v$ is implemented, where λ may be a constant gain or an output error dependent parameter designed to regulate μ around the

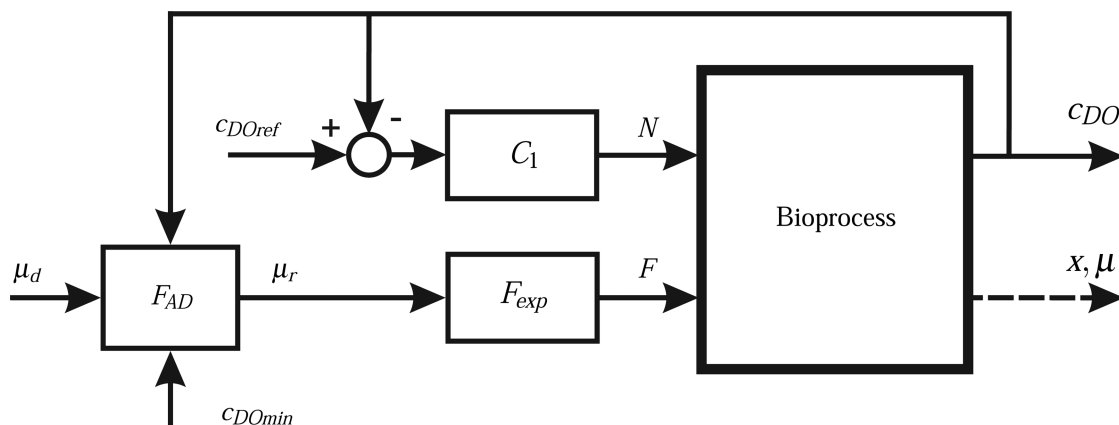


Figure 3. Open-loop exponential feeding law with feeding adaptation block (F_{AD}).

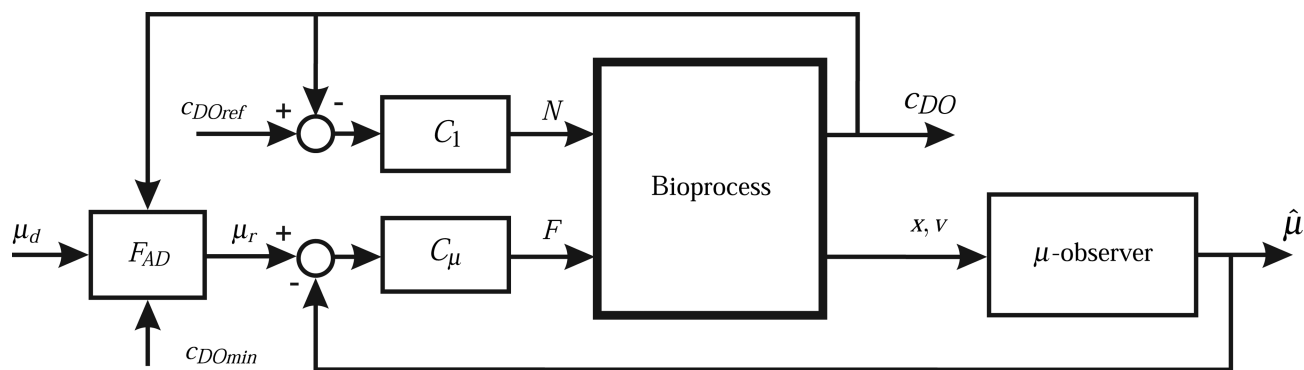


Figure 4. Closed loop control of μ with feeding adaptation: μ -controller (C_μ) and feeding adaptation block (F_{AD}).

desired value. Regarding biomass measurement, equipment based on dielectric spectroscopy and various optical methods have been applied in bioreactors for different microorganisms.^{24,27}

Note that the proposals in Figure 3 and Figure 4 preserve the decentralized structure given in Figure 1. Thus, the feeding adaptation can be applied to existing process setups without major changes.

3.1. SM Feeding Adaptation Algorithm. In the feeding adaptation block, the following function is constructed:

$$S(c_{DO}) = c_{DO} - c_{DOmin} + \tau \dot{c}_{DO} \tag{12}$$

Figure 5 depicts the surface $S(c_{DO}) = 0$ in the phase plane. The idea is to prevent the DO from decreasing faster than the dynamics prescribed by $S = 0$. Thus, the adaptation algorithm keeps inactive whenever the main DO controller is able to regulate DO close to c_{DOref} . On the contrary, when the main DO controller cannot regulate DO at the set-point (e.g., due to saturation or fault of the stirrer), the oxygen decreases possibly reaching the surface $S = 0$. If $S = 0$ is effectively reached, the adaptation algorithm becomes active reducing the reference in such a way that c_{DO} evolves to c_{DOmin} with the dynamics imposed by $S = 0$. That is, a sliding motion on the surface is enforced so that the DO dynamics is driven toward the point $(c_{DO}, \dot{c}_{DO}) = (c_{DOmin}, 0)$.

A diagram of the adaptation algorithm (block F_{AD} in Figure 3 and Figure 4) is presented in Figure 6. In order to robustly enforce the DO dynamics on $S = 0$, a discontinuous input given by

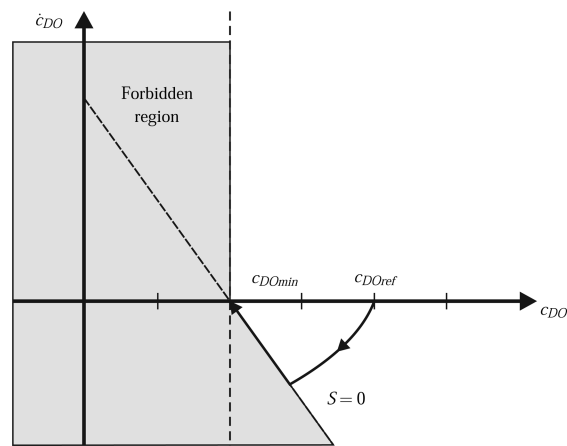


Figure 5. Phase plane of DO and sliding surface.

$$w = \begin{cases} 0 & \text{if } S(c_{DO}) > 0 \\ w_{SM} & \text{otherwise} \end{cases} \tag{13}$$

is applied to reduce the reference value. Note that the control effort is applied only when the DO falls below the surface $S = 0$, i.e. when it is reaching the minimum value or when it is decreasing too fast. This situation leads to a fast switching of w according to the sign of function S in the vicinity of $S = 0$, which can be seen as a transient SM regime on the surface $S = 0$. A first-order low pass filter is applied to smooth out the discontinuous signal, thus the dynamics of μ_r is given by

$$\dot{\mu}_r = -\alpha_f(\mu_r + w - \mu_d), \quad \mu_d > \mu_r \tag{14}$$

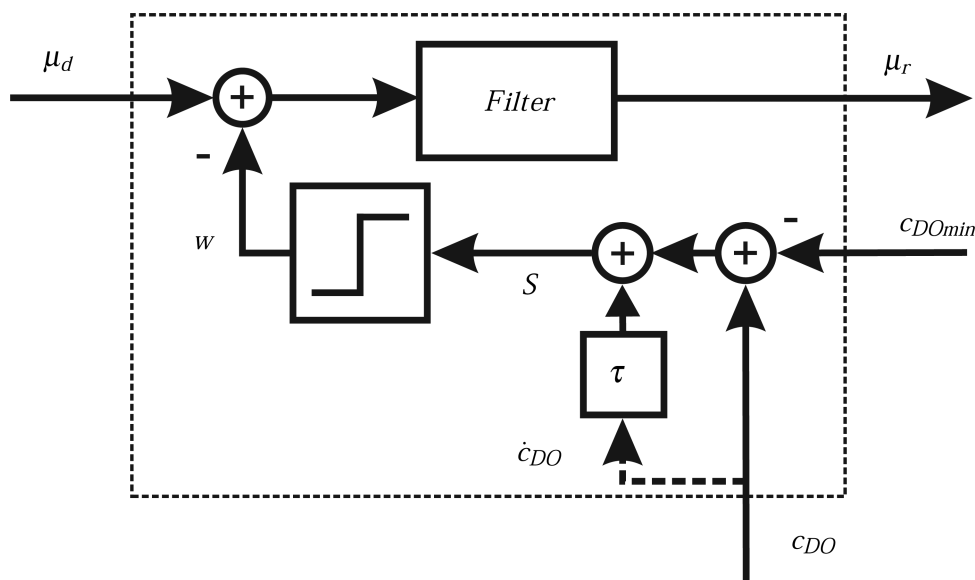


Figure 6. Scheme of feeding adaptation block F_{AD} .

3.2. Analysis of SM Conditions. In order to analyze the SM conditions, the systems under consideration are written in the control-affine form

$$\dot{z} = f(\cdot) + g(z)w \tag{15}$$

with z denoting the whole state vector.

The control law (13) leads to a sliding regime²⁸ on $S(c_{DO}) = 0$ if the following inequalities are locally satisfied

$$\dot{S} = \begin{cases} \nabla S^T f < 0 & \text{if } S(c_{DO}) > 0 \\ \nabla S^T f + \nabla S^T g w_{SM} > 0 & \text{otherwise} \end{cases} \tag{16}$$

where ∇S^T is the gradient of $S(c_{DO})$, and $\nabla S^T f$ denotes the derivative of S along f . The first inequality in (16) holds whenever the DO decreases. From the second inequality, the term $\nabla S^T g w_{SM}$ must be greater than $\nabla S^T f$ in order to force a sign change in the time derivative of S . This is accomplished by selecting w_{SM} high enough. Under this condition, w switches at high frequency enforcing c_{DO} to slide on $S = 0$. The parameter μ_r , so generated is such that the feeding flow fulfills the aerobic condition. Under the SM regime, the expressions

$$S(c_{DO}) = 0 \tag{17a}$$

$$\dot{S}(c_{DO}) = 0 \tag{17b}$$

hold and are known as *invariance condition*.²⁹ Thus, given eq 12, the resulting dynamics for c_{DO} is

$$\dot{c}_{DO} = \frac{c_{DOmin} - c_{DO}}{\tau} \tag{18}$$

Equation 18 describes the dynamics of dissolved oxygen when the system operates in the SM regime. Since the SM regime is established with c_{DO} above the minimum value, the DO decreases toward c_{DOmin} with time constant τ .

Now consider the process described in Figure 3 with the feeding law

$$F_{exp} = \frac{\frac{\mu_r}{Y_{xs}} + m_s}{S_i - s_r} x_0 v_0 e^{\mu_r t} \tag{19}$$

where s_r is the substrate concentration compatible with μ_r (i.e., $\mu(s_r) = \mu_r$). Equation 19 follows by solving eqs 2 and $d(xv)/dt = \mu_r xv$ for $ds/dt = 0$. The main advantage of the feeding law given by eq 19 is its simplicity. However, the initial biomass $x_0 v_0$ and certain parameters must be known. From eqs 1–4, 14, and 19, the state-space equations in form 15 result in

$$\begin{pmatrix} \dot{x} \\ \dot{s} \\ \dot{c}_{DO} \\ \dot{v} \\ \dot{F} \\ \dot{\mu}_r \end{pmatrix} = \begin{pmatrix} \left(\mu - \frac{F}{v}\right)x \\ -q_s x + (S_i - s) \frac{F}{v} \\ OTR - OUR - c_{DO} \frac{F}{v} \\ F \\ -\alpha_f f_s (\mu_r - \mu_d) + g_s \\ -\alpha_f (\mu_r - \mu_d) \end{pmatrix} + \begin{pmatrix} 0 \\ 0 \\ 0 \\ 0 \\ -\alpha_f f_s \\ -\alpha_f \end{pmatrix} w \tag{20}$$

where w is the input (13) and

$$f_s = \left[\frac{1}{Y_{xs}} + \left(\frac{\mu_r}{Y_{xs}} + m_s \right) t \right] x_0 v_0 e^{\mu_r t} \tag{21a}$$

$$g_s = \left(\frac{\mu_r}{Y_{xs}} + m_s \right) \mu_r x_0 v_0 e^{\mu_r t} \tag{21b}$$

Here, the measured output is $y = c_{DO}$. Condition 16 results in

$$\dot{S} = \begin{cases} \nabla S^T f < 0 & \text{if } S(\cdot) > 0 \\ \nabla S^T f + \alpha_f \tau \frac{c_{DO}}{v} f_s w_{SM} > 0 & \text{otherwise} \end{cases} \tag{22}$$

Recalling that the state variables are positive and noting that $f_s \geq x_0 v_0 / Y_{xs}$, it is seen that $\alpha_f \tau (c_{DO}/v) f_s$ is nonzero. This result is in fact a necessary condition for a SM regime. The analysis for a closed-loop configuration can be done in a similar way.

Clearly, the proposed modification to μ_r is easy to implement to the widely used feeding law (19) since no additional process measurements are required. Besides, the block F_{AD} has low

complexity and can be easily implemented in a software routine.

4. RESULTS AND DISCUSSION

Numerical simulations are presented in this section to show the performance of the proposed algorithm. The first case corresponds to the open-loop feeding presented in Figure 3. Since the objective here is to show an improvement of the open-loop approach with respect to DO dynamics, the parameters of eq 19 are assumed known. In the second case, the closed-loop approach presented in Figure 4 is considered under two possible scenarios.

The aerobic bioprocess model (1–4) was used with the parameters for a *P. pastoris* strain presented in Oliveira et al.⁸ The complete list of parameters is given in Table 1 (the maintenance coefficients m_s and m_o are assumed negligible). The initial conditions for fed-batch operation were $x(0) = 10 \text{ g L}^{-1}$, $s(0) = 0.0 \text{ g L}^{-1}$, $c_{DO}(0) = 7 \text{ mg L}^{-1}$, and $v(0) = 15 \text{ L}$. The carbon source was glycerol with $S_i = 500 \text{ g L}^{-1}$. The desired μ was $\mu_d = 0.05 \text{ h}^{-1}$, whereas c_{DOref} was 30% of c_{DO}^* . The minimum DO concentration was set to 20% of c_{DO}^* . The simulation study was performed using Euler's method with a fixed-step of 0.001 h. Additive and multiplicative noise was added in both biomass and DO measurements using filtered (12.5 rad/h) zero-mean Gaussian noise with $\sigma_x = 0.2 \text{ g L}^{-1}$ and $\sigma_{DO} = 0.5 \text{ mg L}^{-1}$, respectively. The DO sensor dynamics was modeled by

$$\dot{c}_{DOs} = -\frac{c_{DOs}}{\tau_{DO}} + \frac{c_{DO}}{\tau_{DO}} \quad (23)$$

with $\tau_{DO} = 20 \text{ s}$.³⁰

The time derivative of c_{DO} required in the switching function (12) was estimated with the SM differentiator presented by Levant³¹

$$\hat{\dot{c}}_{DO}(t) = u_1 + a_1 |\tilde{c}_{DO}|^{1/2} \text{sign}(\tilde{c}_{DO}) \quad (24a)$$

$$\dot{u}_1(t) = a_2 \text{sign}(\tilde{c}_{DO}) \quad (24b)$$

where $\tilde{c}_{DO} \triangleq c_{DOs} - \hat{c}_{DO}$. Algorithm 24 was tuned with $(a_1, a_2) = (8, 6)$ obtained as a trade-off between convergence speed and estimation noise. Note that $\tilde{c}_{DO} \equiv 0$ under SM regime. Therefore, u_1 is an estimate of the DO time derivative.

4.1. Application to Open-Loop Feeding. First, the open-loop feeding law (19) was applied without the feeding adaptation. The results are presented in Figure 7 as a dashed line. During the first 25 h, the process ran with sufficient DO and $\mu \approx \mu_d$ was achieved (Figure 7a). It can be observed in Figure 7f that the stirring speed was increased to maintain the aerobic level. However when N_{max} was reached, the DO started to decrease again (Figure 7b). Consequently, μ diminished due to oxygen limitation, and the exceeding glycerol started to accumulate in the culture (Figure 7d). The objective of maintaining the aerobic level was not accomplished. The results with the proposed auxiliary loop are presented as a solid line. At $t \approx 26 \text{ h}$ the stirrer speed reached N_{max} and the DO started to decrease due to the increasing oxygen demand. Then, the SM loop became active, and the original feeding law was reduced to fulfill the required aerobic level (Figure 7e). As can be observed, $c_{DO} \geq c_{DOmin} = 0.2c_{DO}^*$ was achieved (Figure 7b). Since F_{exp} was reduced to be compatible with the oxygen transfer rate, no glycerol accumulation is observed (Figure 7d).

As can be seen, the proposed algorithm is a simple solution to guarantee the aerobic level in fed-batch bioprocesses. It

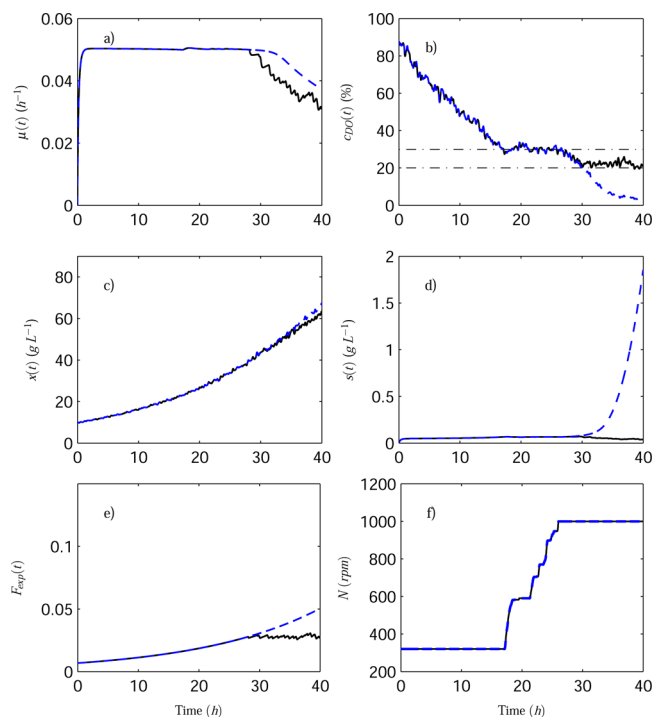


Figure 7. Results obtained with the open-loop feeding law (19): without feeding adaptation (blue dashed line) and with feeding adaptation (solid black line).

provides an enhancement to the open-loop feeding law, only requiring online measurement of DO concentration.

4.2. Application to Closed-Loop Feeding. If biomass and volume measurements are available online, then a wide variety of feedback controllers can be implemented,⁹ for instance, biomass proportional feeding laws of the form

$$F_{expCL} = \lambda xv \quad (25)$$

Here we applied the following nonlinear proportional control law

$$\lambda = \frac{\frac{H}{Y_{xs}} + m_s}{S_i - s_r} (1 - k_c(\hat{\mu} - \mu_r)) \quad (26)$$

where k_c is a constant gain to speed-up the response of the controller, and $\hat{\mu}$ is an estimation of μ .³²

A reduction in OTR may cause the DO concentration to decrease below c_{DOmin} . In this example, the agitation speed was reduced to N_{min} within the interval [22,24.5] h. This could be done for example to reduce foaming. In Figure 8, during the first 22 h the main control loop was able to regulate μ and the DO was about 30%. At $t = 22 \text{ h}$ the agitation speed was set to N_{min} . Without the feeding adaptation algorithm, the DO decreased and μ slightly diminished (Figure 8a). When the agitation speed was restored, the DO increased and μ rose above the set-point. Note that the aerobic condition was not accomplished. With the feeding adaptation, when the DO was reaching c_{DOmin} μ_r was reduced (red dashed line in Figure 8a) in order to reduce the oxygen demand. It is seen that the growth rate (black solid line) closely followed its reference value. At $t = 24.5 \text{ h}$ the stirring speed was increased again, the DO concentration rose, and the SM allowed μ_r to increase. From then on, the feeding adaptation became inactive because

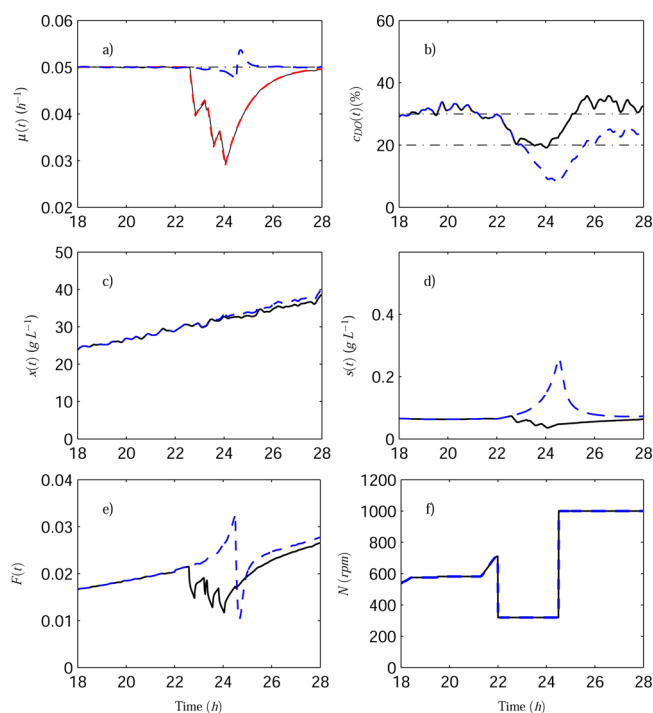


Figure 8. Results obtained with the closed-loop feeding law in the case of partial OTR reduction: without feeding adaptation (blue dashed line) and with feeding adaptation (black solid line). In a) the reference growth rate is shown with a red dashed line overlapping the real growth rate with feeding adaptation.

the aerobic level was greater than c_{DOmin} . Unlike the result without auxiliary loop, no accumulation of glycerol is observed.

Figure 9 presents a case of total failure. If OTR goes to zero, a minimum DO cannot be guaranteed even without growth. However, the feeding adaptation is still useful to improve the transient response until the fault is cleared. Again, when the DO reached a growth limiting level, the response of the μ control loop without feeding adaptation was to add more glycerol into the culture trying to compensate for the decreasing μ . This led to an excess of glycerol in the culture (Figure 9d). By the time the OTR was restored, the DO level increased, and using the glycerol in excess the biomass grew faster than the set-point value. Then the response of the main controller was to reduce the feed (Figure 9e) in order to decrease the growth rate. This shows an undesired response in both μ and s , when the DO concentration becomes the rate-limiting substrate. On the contrary, with the feeding adaptation μ is reduced in a controlled way (Figure 9a), and, consequently, the DO remains below c_{DOmin} for a shorter time interval. Although the DO constraint is not satisfied in this case, the feeding adaptation maintains a low glycerol concentration throughout the cultivation. This is very important in fed-batch cultures since substrate accumulation could lead not only to byproducts formation but also to process instability (e.g., in case of Haldane kinetics).

5. CONCLUSIONS

In this paper, the problem of DO guarantees in aerobic bioprocesses was addressed. A feeding adaptation algorithm based on sliding mode techniques was applied to a decentralized control structure of specific growth rate and DO. The SM algorithm prevents DO from falling faster than a

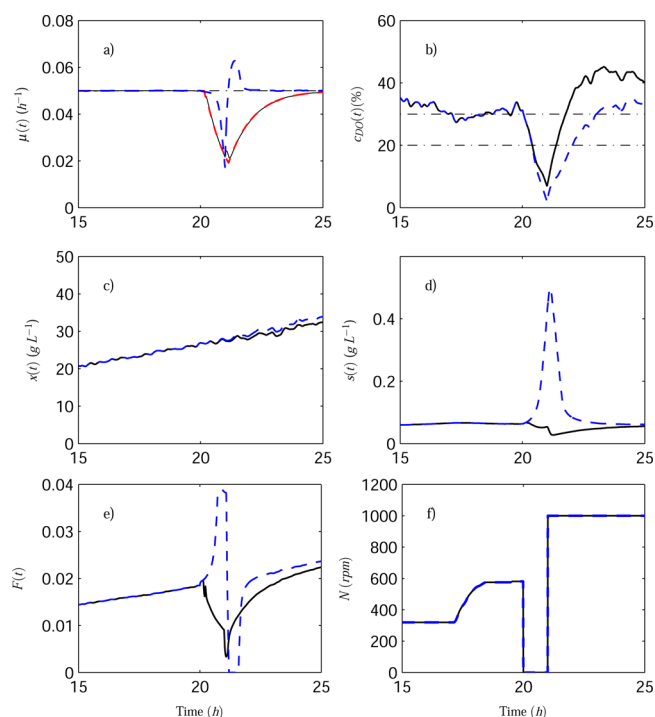


Figure 9. Results obtained with the closed-loop feeding law in the case of total OTR reduction: without feeding adaptation (blue dashed line) and with feeding adaptation (black solid line). In a) the reference growth rate is shown with a red dashed line.

pre-established law in such a way that the DO concentration remains above a prescribed value.

The design and performance of the proposed scheme was illustrated for two relevant feeding policies, the open-loop exponential profile and the closed-loop control of μ , in a *P. pastoris* cultivation. It was shown that undesired substrate accumulation can be circumvented for two typical situations: in high cell density operation and under faulty conditions.

It is important to remark that the proposal does not require additional process measurements and does not depend on the process model. Then, it can also be applied for supervision of pre-existent feeding algorithms.

AUTHOR INFORMATION

Corresponding Author

*Phone: +54 221-425-9306. Fax: +54 221-425-9306. E-mail: sebastian.nuniez@ing.unlp.edu.ar.

Notes

The authors declare no competing financial interest.

ACKNOWLEDGMENTS

This paper was supported by the Agency for the Promotion of Science and Technology ANPCyT (PICT 2011-0888 and PICT 2012-0037), the National Research Council CONICET (PIP 112-2008-01-01052 and PIP 112-2011-01-00361), and the National University of La Plata (Project 11/I164) of Argentina.

NOMENCLATURE

α = agitator parameter 1, $\text{rpm}^{-\beta} \text{h}^{-1}$

β = agitator parameter 2, -

μ = specific growth rate, h^{-1}

μ_{max} = maximum specific growth rate, h^{-1}

OTR = oxygen transfer rate, $\text{g L}^{-1} \text{h}^{-1}$

OUR = oxygen uptake rate, $\text{g L}^{-1} \text{h}^{-1}$
 c_{DO}^* = saturation DO concentration, g L^{-1}
 F = flow rate, L h^{-1}
 $K_L a$ = volumetric mass transfer coefficient for O_2 , h^{-1}
 k_o = half-saturation coefficient for DO, g L^{-1}
 k_s = affinity constant, g L^{-1}
 m_o = oxygen consumption rate for maintenance, $\text{g g}^{-1} \text{h}^{-1}$
 m_s = substrate consumption rate for maintenance, $\text{g g}^{-1} \text{h}^{-1}$
 N = stirrer speed, rpm
 q_s = substrate specific consumption rate, $\text{g g}^{-1} \text{h}^{-1}$
 q_{O_2} = oxygen specific consumption rate, $\text{g g}^{-1} \text{h}^{-1}$
 S_i = influent substrate concentration, g L^{-1}
 Y_{xo} = oxygen to biomass yield, g g^{-1}
 Y_{xs} = substrate to biomass yield, g g^{-1}

REFERENCES

- (1) Soni, A. S.; Parker, R. S. Closed-loop control of fed-batch bioreactors: a shrinking-horizon approach. *Ind. Eng. Chem. Res.* **2004**, *43*, 3381–3393.
- (2) Johnson, A. The control of fed-batch fermentation processes - a survey. *Automatica* **1987**, *23*, 691–705.
- (3) Balsa-Canto, E.; Banga, J. R.; Alonso, A. A.; Vassiliadis, V. S. Efficient optimal control of bioprocesses using second-order information. *Ind. Eng. Chem. Res.* **2000**, *39*, 4287–4295.
- (4) Ren, H.; Yuan, J. Model-based specific growth rate control for *Pichia pastoris* to improve recombinant protein production. *J. Chem. Technol. Biotechnol.* **2005**, *80*, 1268–1272.
- (5) Schenk, J.; Balazs, K.; Jungo, C.; Urfer, J.; Wegmann, C.; Zocchi, A.; Marison, I.; von Stockar, U. Influence of specific growth rate on specific productivity and glycosylation of a recombinant avidin produced by a *Pichia pastoris* Mut⁺ strain. *Biotechnol. Bioeng.* **2008**, *99*, 368–377.
- (6) Potvin, G.; Ahmad, A.; Zhang, Z. Bioprocess engineering aspects of heterologous protein production in *Pichia pastoris*: a review. *Biochem. Eng. J.* **2012**, *64*, 91–105.
- (7) Garelli, F.; Mantz, R. J.; De Battista, H. Partial decoupling of non-minimum phase processes with bounds on the remaining coupling. *Chem. Eng. Sci.* **2006**, *61*, 7706–7716.
- (8) Oliveira, R.; Clemente, J. J.; Cunha, A. E.; Carrondo, M. J. T. Adaptive dissolved oxygen control through the glycerol feeding in a recombinant *Pichia pastoris* cultivation in conditions of oxygen transfer limitation. *J. Biotechnol.* **2005**, *116*, 35–50.
- (9) Bastin, G.; Dochain, D. *On-line Estimation and Adaptive Control of Bioreactors*; Elsevier: 1990.
- (10) Moser, A. *Bioprocess Technology - Kinetics and Reactors. (Revised and Expanded Translation by Philip Manor)*; Springer-Verlag: 1988.
- (11) Pirt, S. J. The maintenance energy of bacteria in growing cultures. *Proc. R. Soc. London, Ser. B* **1965**, *163*, 224–231.
- (12) Özbek, B.; Gayik, S. The studies on the oxygen mass transfer coefficient in a bioreactor. *Process Biochem.* **2001**, *36*, 729–741.
- (13) Chung, Y.; Chien, I.; Chang, D. Multiple-model control strategy for a fed-batch high cell-density culture processing. *J. Process Control* **2006**, *16*, 9–26.
- (14) Schuler, M.; Marison, I. Real-time monitoring and control of microbial bioprocesses with focus on the specific growth rate: current state and perspectives. *Appl. Microbiol. Biotechnol.* **2012**, *94*, 1469–1482.
- (15) Gomes, J.; Menawat, A. S. Precise control of dissolved oxygen in bioreactors - a model-based geometric algorithm. *Chem. Eng. Sci.* **2000**, *55*, 67–78.
- (16) Han, H.-G.; Qiao, J.-F. Adaptive dissolved oxygen control based on dynamic structure neural network. *Appl. Soft. Comput.* **2011**, *11*, 3812–3820.
- (17) Lee, S. C.; Hwang, Y. B.; Chang, H. N.; Chang, Y. K. Adaptive control of dissolved oxygen concentration in a bioreactor. *Biotechnol. Bioeng.* **1991**, *37*, 597–607.
- (18) Ertunc, S.; Akay, B.; Boyacioglu, H.; Hapoglu, H. Self-tuning control of dissolved oxygen concentration in a batch bioreactor. *Food Bioprod. Process.* **2009**, *87*, 46–55.
- (19) Korz, D. J.; Rinas, U.; Hellmuth, K.; Sanders, E. A.; Deckwer, W. D. Simple fed-batch technique for high cell density cultivation of *Escherichia coli*. *J. Biotechnol.* **1995**, *39*, 59–65.
- (20) Inan, M.; Meagher, M. M. The effect of ethanol and acetate on protein expression in *Pichia pastoris*. *J. Biosci. Bioeng.* **2001**, *92*, 337–341.
- (21) Lim, H.-K.; Choi, S.-J.; Kim, K.-Y.; Jung, K.-H. Dissolved-oxygen-stat controlling two variables for methanol induction of rGuamerin in *Pichia pastoris* and its application to repeated fed-batch. *Appl. Microbiol. Biotechnol.* **2003**, *62*, 342–348.
- (22) Alford, J. S. Bioprocess control: advances and challenges. *Comput. Chem. Eng.* **2006**, *30*, 1464–1475.
- (23) Dochain, D. State and parameter estimation in chemical and biochemical processes: a tutorial. *J. Process Control* **2003**, *13*, 801–818.
- (24) Claes, J. E.; Van Impe, J. F. On-line estimation of the specific growth rate based on viable biomass measurements: experimental validation. *Bioprocess Eng.* **1999**, *21*, 389–395.
- (25) De Battista, H.; Picó, J.; Garelli, F.; Navarro, J. L. Reaction rate reconstruction from biomass concentration measurement in bioreactors using modified second-order sliding mode algorithms. *Bioprocess Biosyst. Eng.* **2012**, *35*, 1615–1625.
- (26) Mohseni, S. S.; Babaeipour, V.; Vali, A. R. Design of sliding mode controller for the optimal control of fed-batch cultivation of recombinant *E. coli*. *Chem. Eng. Sci.* **2009**, *64*, 4433–4441.
- (27) Kiviharju, K.; Salonen, K.; Moilanen, U.; Eerikäinen, T. Biomass measurement online: the performance of in situ measurements and software sensors. *J. Ind. Microbiol. Biotechnol.* **2008**, *35*, 657–665.
- (28) Edwards, C.; Spurgeon, S. K. *Sliding Mode Control: Theory and Applications*, 1st ed.; Taylor & Francis: UK, 1998.
- (29) Utkin, V.; Guldner, J.; Shi, J. *Sliding Mode Control in Electromechanical Systems*, 1st ed.; Taylor & Francis: London, 1999.
- (30) Soons, Z.; Voogt, J.; van Straten, G.; van Boxtel, A. Constant specific growth rate in fed-batch cultivation of *Bordetella pertussis* using adaptive control. *J. Biotechnol.* **2006**, *125*, 252–268.
- (31) Levant, A. Robust exact differentiation via sliding mode technique. *Automatica* **1998**, *34*, 379–384.
- (32) De Battista, H.; Picó, J.; Picó-Marco, E. Nonlinear PI control of fed-batch processes for growth rate regulation. *J. Process Control* **2012**, *22*, 789–797.

NOTE ADDED AFTER ASAP PUBLICATION

After this paper was published online December 3, 2013, a correction was made to the text below eq 24b. The corrected version was reposted December 5, 2013.